ECAS 2022

MDPI

Proceedings

Application of a local three-dimensional (3D) atmospheric model for description of carbon dioxide exchange over a non-uniform land surface †

Iuliia Mukhartova [1,*], Julia Kurbatova [2] and Alexander Olchev [1]

1 Department of Meteorology and Climatology, Lomonosov Moscow State University, Moscow, Russia; muhartova@yandex.ru
2 A.N. Severtsov Institute of Ecology and Evolution, Russian Academy of Science, Moscow, Russia
* Correspondence: muhartova@yandex.ru;
† Presented at The 5th International Electronic Conference on Atmospheric Sciences (ECAS 2022) on 16-31 July, 2022.

Abstract: The three-dimensional hydrodynamic model was developed to describe the turbulent transfer of carbon dioxide (CO_2) within the atmospheric surface layer taking into account the horizontal land surface heterogeneity. It is based on the "one and a half" E–ω closure for the system of averaged Navier-Stokes and continuity equations. The model was applied to assess the spatial wind and atmospheric CO_2 flux distribution in a non-uniform forest peatland ecosystem in Central part of European Russia. The modeling results showed a very strong spatial heterogeneity of wind speed and atmospheric CO_2 fluxes. They also showed a very good agreement with the results of eddy covariance flux measurements.

Keywords: atmospheric surface layer, Navier-Stokes and continuity equations, three-dimensional (3D) model, surface heterogeneity, peatland ecosystem.

Academic Editor: Andreas Matzarakis

Published: 20 July 2022

Publisher's Note: MDPI stays neutral with regard to jurisdictional claims in published maps and institutional affiliations.

1. Introduction

Modern climate changes are accompanied by a strong increase in global temperature, changes of the precipitation patterns, increase of the frequency and severity of extreme weather events. Most experts of climate change are associated these changes with an increase in concentrations of greenhouse gases (GHG) in the atmosphere coming mainly from various anthropogenic sources. Natural ecosystems influence actively the concentrations of GHG (CO_2, CH_4, N_2O, etc.) in the atmosphere. In particular, the natural ecosystems, on the one hand, release CO_2 into the atmosphere through the autotrophic and heterotrophic respiration, and on the other hand, they absorb actively CO_2 from the atmosphere during photosynthesis. The reliable knowledge on GHG fluxes in natural ecosystems is obviously very important for adequate projection of modern and future climate change.

A wide range of experimental methods are currently used to determine GHG fluxes between land surface and the atmosphere. The eddy covariance technique as a most widely used method in the world practice for flux measurements, however, has many limitations for the broader application [1]. In particular, a significant limitation of the eddy covariance method is a required homogeneity of vegetation canopy and surface topography, that is rarely observed under natural conditions. Process-based mathematical models for the GHG transfer can be very effective tools for describing the fluxes between heterogeneous land surface and the atmosphere.

The modern models of GHG transfer have different levels of complexity and use different approximations and simplifications for description of vegetation properties [2-4].

The most models describing the air flow distribution within the atmospheric surface layer are based on the system of the Navier-Stokes and continuity equations. In order to simplify the computational procedure, most existing models apply the Reynolds decomposition. Additional equations expressing unknown values through high-order moments are usually used to close the averaged system of equations [5].

The simplest way to close a system of averaged equations is based on the Boussinesq conjecture, according to which a turbulent flux of some substance is assumed to be similar to molecular transport and proportional to a gradient of this substance. Presently, there are many models for describing the momentum transfer in the atmosphere (e.g. Large Eddy simulation (LES) models [6]), and there are very few local models of mid-level complexity that allow us to describe operationally the GHG transfer within the atmospheric surface layer taking into account the possible sinks and sources.

The main goal of the study is to develop a 3D model of turbulent transfer of GHG over a non-uniform land surface within the atmospheric surface layer, and apply it to describe the spatial wind and CO_2 flux distributions above a non-uniform forest peat-land "Staroselsky Moch" in Central part of European Russia.

2. Materials and Methods

2.1. System of equations for velocity components and turbulent exchange coefficient.

For the wind velocity vector $\vec{V} = \{u, v, w\}$, we use the Reynolds decomposition $\vec{V} = \bar{\vec{V}} + \vec{V}'$ separating the average component $\bar{\vec{V}}$ and the "fluctuating" component $\vec{V}'$ with zero average. In used approximation, the air is considered to be incompressible. In the case of neutral atmospheric stratification, average wind velocity $\bar{\vec{V}}$ satisfies the following system of equations [7]:

$$\frac{\partial \bar{\vec{V}}}{\partial t} + \left(\bar{\vec{V}}, \nabla\right)\bar{\vec{V}} = -\frac{1}{\rho}\nabla P - \overline{\left(\nabla, \vec{V}'\right)\vec{V}'} + \vec{F}_{cor} + \vec{F}_d + \vec{g}\,, \qquad \operatorname{div}\bar{\vec{V}} = 0\,, \tag{1}$$

where ρ is the average air density, P is the pressure, $\vec{g}$ is the acceleration of gravity, $\vec{F}_{cor}$ and $\vec{F}_d$ are the specific forces of Coriolis and vegetation resistance, respectively.
The specific resistance force of vegetation can be parameterized as follows [8]:

$$\vec{F}_d = -c_d \cdot PLAD \cdot \left|\bar{\vec{V}}\right| \cdot \bar{\vec{V}}\,,$$

where c_d is a dimensionless coefficient of vegetation resistance, $PLAD(x,y,z)$ is the phytomass density, which includes both foliage (*LAD*) and non-photosynthetic (*SAD*) elements of plants (branches, trunks): *PLAD=LAD+SAD*.

In our model, we use the so-called "one-and-a-half" closure scheme and the Boussinesq hypothesis [3, 9] to parameterize the turbulent fluxes $\overline{u'\vec{V}'}$, $\overline{v'\vec{V}'}$ and $\overline{w'\vec{V}'}$:

$$\overline{(u')^2} = \frac{2}{3}E - 2K\frac{\partial \bar{u}}{\partial x}, \quad \overline{(v')^2} = \frac{2}{3}E - 2K\frac{\partial \bar{v}}{\partial y}, \quad \overline{(w')^2} = \frac{2}{3}E - 2K\frac{\partial \bar{w}}{\partial z},$$

$$\overline{u'v'} = -K\left(\frac{\partial \bar{u}}{\partial y} + \frac{\partial \bar{v}}{\partial x}\right), \quad \overline{u'w'} = -K\left(\frac{\partial \bar{u}}{\partial z} + \frac{\partial \bar{w}}{\partial x}\right), \quad \overline{v'w'} = -K\left(\frac{\partial \bar{v}}{\partial z} + \frac{\partial \bar{w}}{\partial y}\right),$$

where E is the turbulent kinetic energy (TKE), K is the turbulent exchange coefficient. One-and-a-half order closure (or two equation closure) assumes that the coefficient K is calculated using the TKE and its dissipation rate ε: $K = C_\mu E^2/\varepsilon$, and the functions E and $\omega = \varepsilon/E$ satisfy the diffusion-reaction-advection type equations [3, 9].

2.2. Initial and boundary conditions for the dynamical part of the model.

The system of equations (1) is solved in a rectangular domain as a problem of establishing with some initial wind distribution. The initial and boundary conditions are consistent with a classical "one-dimensional" model describing a turbulent conditions over a horizontally homogeneous surface:

$$V_0(z)=\frac{u_*}{\kappa}\ln\frac{z}{z_0},\quad \bar{u}\big|_{t=0}=V_0(z)\sin\alpha,\quad \bar{v}\big|_{t=0}=V_0(z)\cos\alpha,\quad \bar{w}\big|_{t=0}=0,$$

where α is the angle between the direction to the north and the average wind direction, u_* is the friction velocity, κ is von Kármán constant, z_0 is the minimum value of the surface roughness layer within the modeling area. The upper boundary conditions are [10]:

$$\left.\frac{\partial\bar{u}}{\partial z}\right|_{z=H}=\left.\frac{\omega}{\sqrt{C_\mu}}\right|_{z=H}\sin\alpha,\quad \left.\frac{\partial\bar{v}}{\partial z}\right|_{z=H}=\left.\frac{\omega}{\sqrt{C_\mu}}\right|_{z=H}\cos\alpha,\quad \left.\frac{\partial\bar{w}}{\partial z}\right|_{z=H}=0$$

.

At the lower boundary of modeling domain a zero velocity is assumed. For the vertical component of wind velocity at the lateral boundaries, we use zero Neumann condition. To set the lateral boundary conditions for the horizontal wind velocity components, we divide the lateral boundary into the "windward" and "leeward or free" parts, depending on the wind direction. At the input boundaries, the horizontal wind velocity is considered to be known, at the leeward boundaries, we use zero Neumann conditions. The initial and boundary conditions for *E* and ω are also consistent with the expressions corresponding to logarithmic wind profile [9-10].

2.3. GHG transport and its fluxes.

The spatial distribution of the GHG concentration $C(x,y,z,t)$ (carbon dioxide CO_2 in our study), is obtained from the diffusion-advection equation:

$$\frac{\partial C}{\partial t}+\left(\bar{\vec{V}},\nabla\right)C=\mathrm{div}\left(K_C\nabla C\right)+F_b-F_{ph},\qquad(2)$$

where K_C is the coefficient of turbulent diffusion for *C*, the term F_b describes the C sources, and the term F_{ph} describes its sinks. CO_2 sources are associated with plant and soil respiration, so the term F_b is the sum of plant canopy (F_b^p) and soil (F_b^s) respiration, and sinks are caused by the absorption of CO_2 during photosynthesis. To parameterize photosynthesis rate, we use the Ball model [11] in Learning's modification [12]:

$$F_{ph}=\frac{LAD}{a}\left(g_s-g_0\right)\left(C-\Gamma_*\right)\left(1+\frac{D_s}{D_0}\right),$$

where *a* and D_0 are empirical coefficients, g_s is the leaf stomatal CO_2 conductance [13]:

$$g_s\left(PAR\right)=g_s^{\max}\left(1-e^{-\beta_s PAR}\right),$$

g_0 is the value of leaf stomatal conductance at the light compensation point, Γ_* is the compensation point for CO_2 concentration, D_s is water vapor pressure deficit.

Turbulent and advective fluxes of the tracer can be estimated as follows:

$$\vec{q}^{turb}=\overline{\vec{V}'C'}=-K_C\nabla C,\quad q_x^{adv}=\bar{u}\,\mathrm{sgn}\left(\bar{u}\right)\frac{\partial C}{\partial x},\quad q_y^{adv}=\bar{v}\,\mathrm{sgn}\left(\bar{v}\right)\frac{\partial C}{\partial y},\quad q_z^{adv}=\bar{w}\,\mathrm{sgn}\left(\bar{w}\right)\frac{\partial C}{\partial z},$$

where $\mathrm{sgn}(\cdot)$ is the sign function equal to 1 if the expression in parentheses is positive, minus 1 if it is negative, and zero if the expression in parentheses is 0.

2.3. The study site.

The peatland "Staroselsky Moch" (Figure 1) selected for our study is situated in the area of sustainable management of the Central Forest State Natural Biosphere Reserve (CFSNBR) (56.473 ° N, 33.041 ° E). The modeling domain includes both the peatland and surrounding forest and grassland landscapes. The total area of modeling domain is about 4 km^2. The surface of the peatland is quite flat with a small slope to the east (less than 1 °).

The peatland belongs to the oligotrophic type, has irregular shape and is characterized by mosaic vegetation.

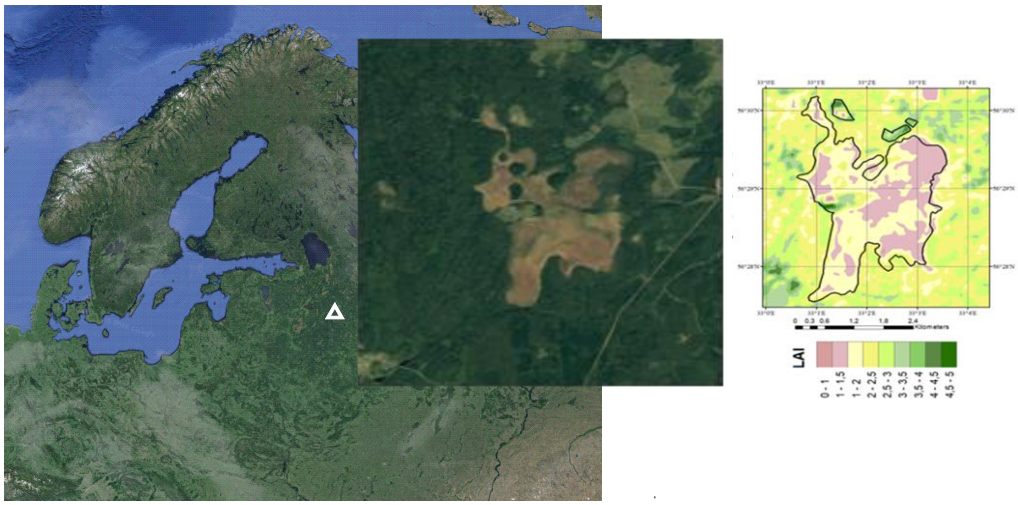

Figure 1. Geographical location of the study area and the spatial pattern of the leaf area index (LAI) within the modeling domain derived from Landsat imagery.

Equipment for meteorological and eddy covariance flux measurements was mounted at a height of 2.4 m on a 3 m tall steel tripod installed in the central part of the peatland. The eddy covariance equipment for measurements of vertical *NEE*, *LE* and *H* fluxes included an open path CO_2/H_2O gas analyzer LI-7500A (LI-COR Inc., USA) and 3-D ultrasonic anemometer CSAT3 (Campbell Scientific, USA). Eddy covariance data were collected at a 10 Hz rate..

3. Results and Discussion

The results of numerical experiments showed a very strong variability of wind components and CO_2 fluxes within the modeling domain. Figure 2 shows a few examples of spatial distribution of vertical and horizontal wind components at different height above a ground surface. Examples of model simulations of vertical and horizontal CO_2 fluxes are shown in Figure 3.

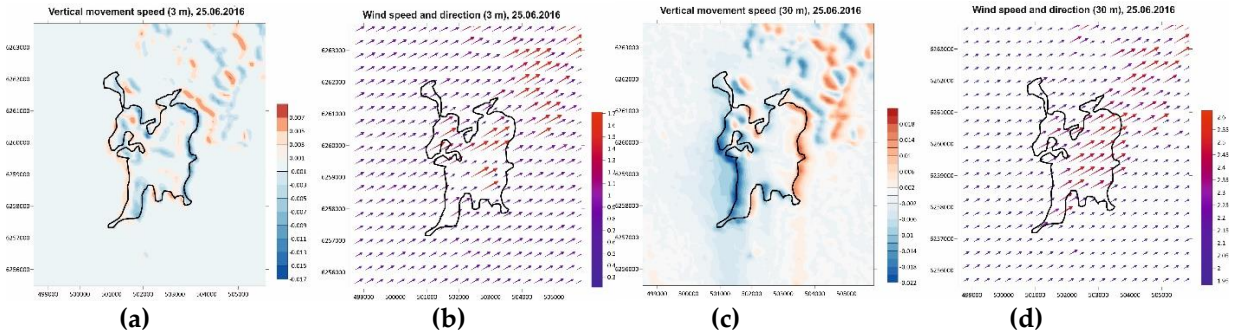

Figure 2. Spatial distributions of vertical and horizontal wind components at the heights of 3 m; (a, **c**) and (b, **d**). For calculation the weather conditions observed at 14:00 on 06/25/2016 were used. The prevailing wind direction at the upper boundary of modeling domain is southeast.

The mosaic and heterogeneous structure of a plant canopy results in a large heterogeneity of spatial wind distribution. The largest anomalies of vertical wind components were found at the boundaries of various communities, and particularly at wind- and leeward forest boundaries. The modeling results showed, at the same time, insignificant changes of wind direction at different heights above the ground surface. It was shown the

downward air flows at the windward and upward air flows at leeward forest boundaries at the 3m height above a ground surface. The vertical air flows at the height 30 m (above tree crowns) have opposite directions.

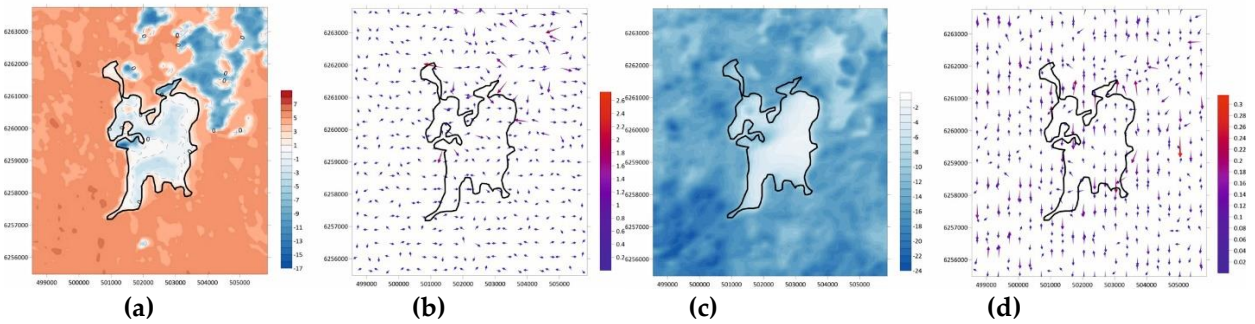

Figure 3. Vertical CO_2 flux at a height of 3 m (**a**) and 30 m (**c**) as well as the horizontal CO_2 fluxes at the height of 3 m (**b**) and 30 m (**d**) above the surface. Calculations conducted for 14:00 on 06/25/2016. CO_2 fluxes are expressed in μmol m^{-2} s^{-1}.

Comparisons of modeled and measured (eddy covariance) vertical CO_2 fluxes in the central part of peatland at the flux tower location and at the height of 3 m above the surface showed a very good agreement between modeled and measured fluxes. At the same time the modeled vertical CO_2 fluxes at the height 30 m above a ground surface are some larger comparing with eddy flux measurement at 3 m level. It is obviously resulted from horizontal CO_2 advection from surrounding forests. In particular, the modeling results showed that whereas the vertical fluxes above a forest canopy at 30 m height is ranged between -12 and -24 μmol m^{-2} s^{-1}, the vertical CO_2 fluxes above the peatland is some smaller and varied in the central part between -2 μmol m^{-2} s^{-1} and -12 μmol m^{-2} s^{-1}, that is some higher than at the lower modeling layers (e.g. 3 m).

The large spatial flux heterogeneity makes very difficult the up-scaling of point flux measurement (e.g. eddy covariance) to entire peatland area. The modeling results show a large difference between calculated vertical CO_2 flux profiles at flux tower site and the averaged vertical CO_2 flux profiles calculated by intergrating of local profiles over the entire peatland area (Figure 4). The difference between flux tower and entire peatland profiles is changed depending on the height above the ground surface and prevailed wind direction.

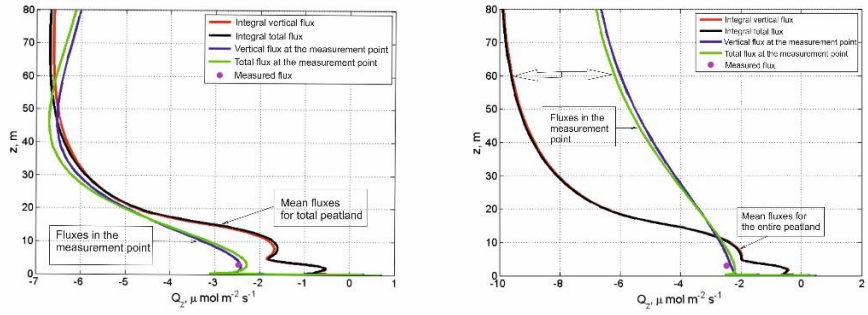

Figure 4. Comparisons of the local flux tower and mean peatland CO_2 fluxes at different levels above a ground surface under (a) south-east (14:00 on 06/25/2016) and (**b**) the northwest wind directions (13:30 on 06/28/2016). The blue line is the total vertical CO_2 fluxes; the green line is a sum of total vertical and horizontal fluxes at flux tower site; the red line is mean vertical flux averaged for the entire peatland area; the black line is a sum of vertical and horizontal fluxes averaged for the entire peatland area.

4. Conclusions

A hydrodynamic model was developed and applied to describe the spatial patterns of wind velocity and vertical and horizontal CO_2 fluxes above a spatially inhomogeneous

peatland "Staroselsky Moch". The results showed a significant heterogeneity of the air flow distributions within both the peatland and surrounding forest. The sharpest changes of vertical and horizontal wind components were found at the windward and leeward forest edges. At the forest edges the maximum rates of horizontal CO_2 fluxes were also detected.

Comparisons of modeled fluxes for the central part of peatland with eddy covariance flux measurements showed a good agreement. A large spatial vegetation heterogeneity within the peatland, and non-uniform surrounding forest makes impossible the simple extrapolation of eddy covariance data to the entire peatland area. The 3D model in the case can be a very effective tool for regional flux up-scaling.

Author Contributions: Conceptualization, A.O. and Iu.M.; methodology, A.O., Iu.M. and J.K.; software, Iu.M.; validation, Iu.M.; investigation, Iu.M., A.O., and J.K.; data curation, J.K. and A.O.; writing—original draft preparation, Iu.M.; writing—review and editing, A.O.; visualization, Iu.M. supervision, A.O.; project administration, A.O.; funding acquisition, A.O. All authors have read and agreed to the published version of the manuscript.

Funding: This research was funded by Lomonosov Moscow State University (grant number AAAA-A16-116032810086-4)

Institutional Review Board Statement: Not applicable

Data Availability Statement: The data obtained in the study can be requested from the authors at muhartova@yandex.ru

Conflicts of Interest: The authors declare no conflict of interest

References

1. Aubinet, M.; Vesala, T.; Papale, D. Eddy Covariance: A Practical Guide to Measurement and Data Analysis. 2012, Dordrecht, The Netherlands: Springer, 438 p.
2. Sellers P., Dickinson R. E., Randall D. A., et al. Modeling the exchanges of energy, water, and carbon between continents and the atmosphere. Science. 1997. 275. P. 502-509
3. Vager, B.; Nadezhina, E. Atmospheric boundary layer in conditions of horizontal non-uniformity Publisher: Gidrometeoizdat., Leningrad, USSR, 1979 (In Russian).
4. Penenko, V.; Aloyan, A. Models and methods for environmental protection problems, Science Publ., Moscow, USSR, 1985 (In Russian).
5. Sogachev, A.; Panferov, O. Modification of two-equation models to account for plant drug. Bound. Lay. Meteorol. 2006, 121(2), pp. 229-266.
6. Sullivan, P.P.; McWilliams, J.C.; Moeng, C.-H. A subgrid-scale model for large-eddy simulation of planetary boundary-layer flows. Boundary-Layer Meteorology. 1994 71 (3), 247–276
7. Wyngaard, J.C. Turbulence in the Atmosphere Publisher: Cambridge University Press, UK, 2010.
8. Dubov, A.S., Bykova, L.P., Marunich, S.V. Turbulence in Vegetation Canopy Publisher: Gidrometeoizdat., Leningrad, USSR, 1978 (In Russian).
9. Mukhartova, Yu.V.; Dyachenko, M.S.; Mangura, P.A.; Mamkin, V.V.; Kurbatova, J.A.; Olchev, A.V. Application of a three-dimensional model to assess the effect of clear-cutting on carbon dioxide exchange at the soil-vegetation-atmosphere interface. IOP Conf. Series: Earth and Environmental Science 2019, 368, 012036.
10. Mukhartova, Yu.V.; Mangura, P.A.; Levashova, N.T.; Olchev, A.V. Selection of boundary conditions for modeling the turbulent exchange process within the atmospheric surface layer. Computer Research and Modeling 2018, 10(1), 27-46 (In Russian).
11. Ball, J.T.; Woodrow, I.E.; Berry, J.A. A model predicting stomatal conductance and its contribution to the control of photosynthesis under different environmental conditions. Progress in Photosynthesis Research 1987, pp. 221-224
12. Leuning, R. A critical appraisal of a combined stomatal-photosynthesis model for C3 plants. Plant Cell Environ. 1995, 18(4), pp. 339-355
13. Oltchev, A.; Ibrom, A.; Constantin, J.; Falk, M.; Richter, I.; Morgenstern, K.; Joo, Y.; Kreilein, H.; Gravenhorst, G. Stomatal and surface conductance of a spruce forest: Model simulation and field measurements. J. Phys. Chem. Earth. 1998, 23(4), pp. 453-458.